

**Central Library**  
**Prince of Songkla University**

Chapter 3

**Results and Discussions**

**3.1 Optimization of gas chromatographic condition**

Instrumental analysis was carried out by using a mass spectrometer (Agilent 5973 MSD, USA) coupled to a GC 6890 series (Agilent Instrument, USA) where a fused silica capillary columns was used (HP-5MS of 30 m X 0.25 mm i.d., film thickness 0.25 μm). This was chosen followed the report by Abad, *et al.* (1997) that 2,3,7,8-TCDD were well-resolved on a DB-5MS, which is equivalent to HP-5MS, and provided an improvement to the resolution of some 2,3,7,8-chloro-substituted PCDDs.

To achieve chromatographic optimum conditions, the following parameters were optimized.

**3.1.1 Carrier gas flow rate**

The optimum carrier gas flow rate can be obtained from a van Deemter plot at the lowest HETP, which provided the highest column efficiency. The van Deemter equation is used for describing the gas chromatographic process. The equation was derived from the consideration of the resistance to mass transfer between the two phases as arising from diffusion. The general form for the van Deemter equation is:

$$h = \text{HETP} = A + B/u + Cu \quad \dots\dots\dots(4)$$

Where  $A = 2\lambda d_p$  = eddy diffusion term;  $d_p$  is the diameter of support particles and  $\lambda$  is a "packing term".

$B = 2\lambda D_g$  = longitudinal or ordinary diffusion term;  $D_g$  is the diffusivity of sample in carrier gas.

$C = (8/\pi^2) [k' / (1+k')^2] (d_f^2 / D_l)$  = nonequilibrium or resistance to mass-transfer term;  $k'$  is the capacity factor (ratio of amount of

sample in stationary phase to amount in carrier gas in a given segment of column),  $d_f$  is the effective film thickness of liquid phase and  $D_l$  is the diffusivity of sample in liquid phase.

$u =$  the linear velocity of carrier gas, cm/s

Equation 4 (Grob, 1985) shows that HETP,  $h$ , is depended on the carrier gas flow rate,  $u$ . This equation represents a hyperbola that has a minimum at velocity  $u = (B/C)^{1/2}$  and a minimum  $h$  value ( $h_{min}$ ) at  $A + 2(BC)^{1/2}$  as illustrated in Figure 5.

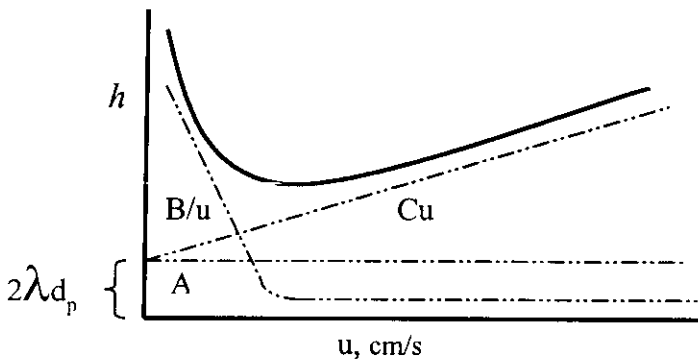


Figure 5 The van Deemter plot changes in  $h$  versus linear gas velocity  $u$ :

$$h_{min} = A + 2(BC)^{1/2} ; u_{pot} = (BC)^{1/2} \text{ (Grob, 1985)}$$

For this experiment, we used a capillary column so there is only one flow path and no packing material. The resistance-to-mass transfer term  $C$  has the greatest effect on band broadening, and its effect in capillary column is controlled by mass transfer in the gas phase  $C_G$ . The  $A$  term, eddy diffusion term, is nonexistent. Then, van Deemter equation is modified to

$$h = B/u + C_G u \quad \dots\dots(5)$$

In practice it is difficult to know the terms of B and C in equation 5. Since HETP is related to the number of theoretical plates, n, and knowing the length of the column, so HETP can be expressed as.

$$h = \text{HETP} = L / n \quad \dots\dots(6)$$

Where L = the column length.

n = the number of the theoretical plates

The total number of theoretical plates, n, influences the degree of peak's resolution. Column efficiency, express as the number of plates per foot n/L, could also be expressed as h, the length of column in millimeters equivalent to one theoretical plate. The lower the h value, the greater the column efficiency. The number of theoretical plates can be calculated from equation 7.

$$n = 16 (t_r/W)^2 \quad \dots\dots(7)$$

Where  $t_r$  is the retention time of peak.

W is the width between the tangents to that peak, at the baseline intercept (Figure 6)

In this work, the number of plates was measured at the bandwidth at half-height,

$W_{1/2}$

$$W = (2/\ln 2)^{1/2} W_{1/2} \quad \dots\dots(8)$$

Combining equation (7) and (8), then

$$\begin{aligned} n &= 8 \ln 2 (V_R/W_{1/2})^2 \\ &= 8(2.30 \log 2)(V_R/W_{1/2})^2 \end{aligned}$$

$$n = 5.54 [V_R / W_{1/2}]^2 \quad \dots\dots\dots(9)$$

Equation (9) was used to calculate  $n$  and HETP was then calculated using equation (6).

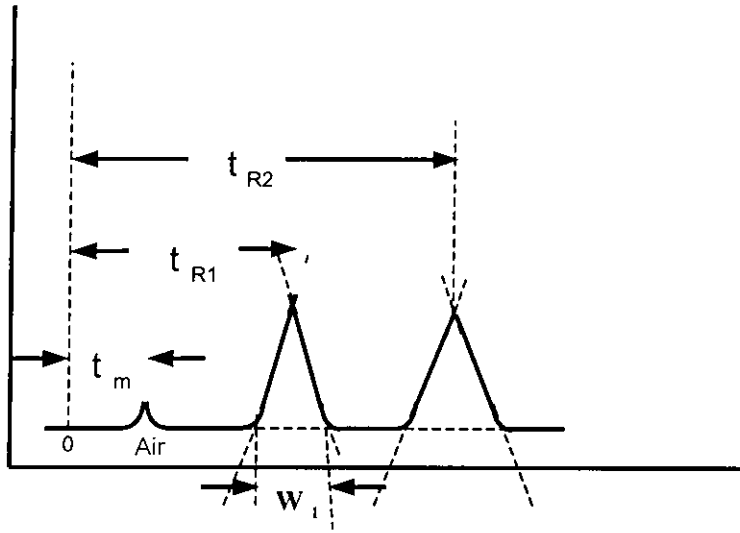


Figure 6 Measurements used in calculating total theoretical plate.

Since this experiment used Mass Selective Detector as the detector of the gas chromatograph, a vacuum sufficient for effective mass spectrometer operation was necessary. To achieve this condition, total column flow rate could not be more than 2 ml/minute. Value of retention time and  $h$ , HETP, at different gas flow rates are shown in Table 6. The optimum carrier gas flow rate for HP-5MS capillary column can be obtained from minimum HETP of the van Deemter plot as shown in Figure 5. HETP decrease when the carrier gas flow rate was varied from 0.7 to 1.0 mL/min and increased with a faster flow rate, when carrier gas flow rate was higher than 1.5 mL/min fluctuated HETP values were obtain. The minimum HETP from figure 5, the lowest point of van Deemter plot, is 1.0 mL/min. The number of theoretical plates at various carrier gas flow rates are shown in Table 7. It indicates that the numbers of theoretical plates at optimum carrier gas flow rate of 638298, the highest value. The more the numbers of plates the higher resolution it takes. This higher resolution is useful to have a three - to tenfold decrease in analysis

time compared with analysis times using packed columns (Grob, 1985) and to provide the ability to separate complex mixtures.

Table 6 Relationship of carrier gas flow rate, HETP and retention time

Carrier gas flow rate ( mL/min )	HETP ( $\times 10^{-3}$ m )	Retention time ( minutes )
0.7	0.057	15.05
0.9	0.048	13.84
1.0	0.047	13.56
1.1	0.048	13.32
1.3	0.052	12.92
1.5	0.057	12.59

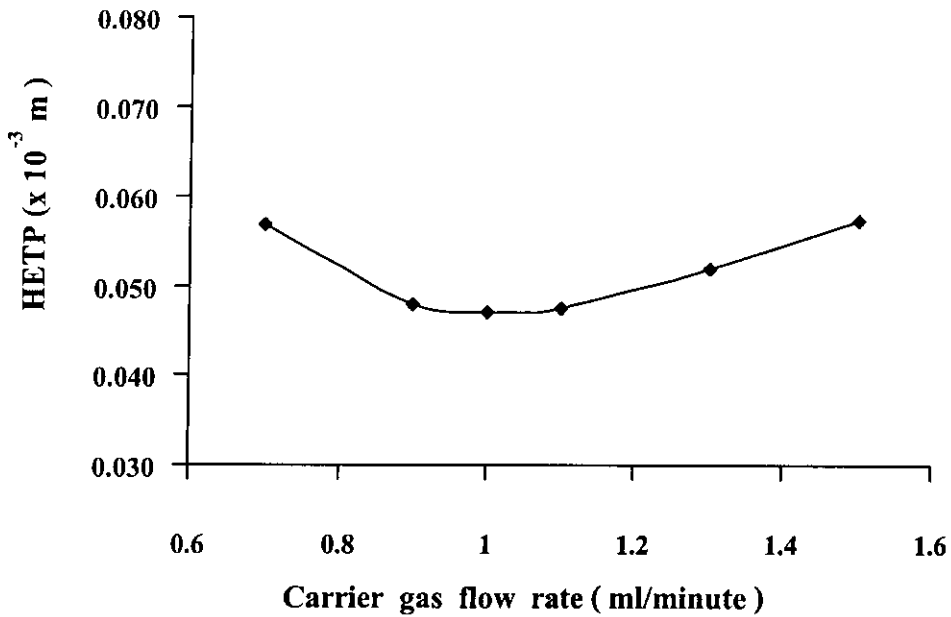


Figure 7 The van Deemter Plot

Table 7 The number of theoretical plates at various carrier gas flow rates

Carrier gas flow rate ( mL/min )	The number of theoretical plates
0.7	526316
0.9	625000
1.0	638298
1.1	625000
1.3	576923
1.5	526316

### 3.1.2 Temperature programming

The column temperature for the analysis must be optimized in the development of analysis method. The column temperature scheme for this study adopted from the US EPA column program ( EPA, 1996 ). The results from column temperature programming studied as in 2.2.1.2 were considered by balancing between the time of analysis and the response. It consisted of 9 steps as follows.

#### Step 1 : Initial temperature

The initial temperature was studied in 2.2.1.2 between 80 to 140°C while other temperatures in the program were fixed as shown in Figure 8.

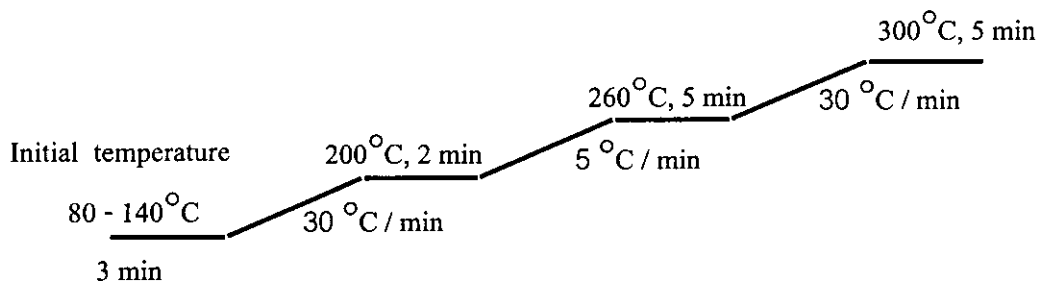


Figure 8 Temperature programming in step 1

The results (Table 8 and Figure 9) showed that the responses slightly decreased as the initial temperatures increased from 80 °C to 90 °C and increased when the temperature increased from 90 °C to 100 °C. It then decreased again when the temperature increased from 100 °C to 140 °C. Since the maximum response was obtained at the initial temperature of 100 °C and there was not much differences of both resolution and analysis time between the different initial temperatures the temperature at 100 °C was chosen. This agreed with Abad *et al.* (1997) who compared the response of TCDD on various types of column ( for example DB- 5MS, DB-5, DB-DIOXIN ) and found that a DB-5MS provided an improvement to the resolution of some 2,3,7,8-chloro-substituted PCDDs with initial temperature of 100 °C.

Table 8 Relative response of MSD detector to various initial temperatures

<b>Initial temperature ( ° C )</b>	<b>Response* ( Abundance )</b>	<b>Analysis times ( minutes )</b>
80	471288	25.67
90	470351	25.34
95	471156	25.17
100	480109	25.00
110	470404	24.67
120	459966	24.34
130	460108	24.00
140	450068	23.67

\*mean of 5 replications, RSD < 4 %

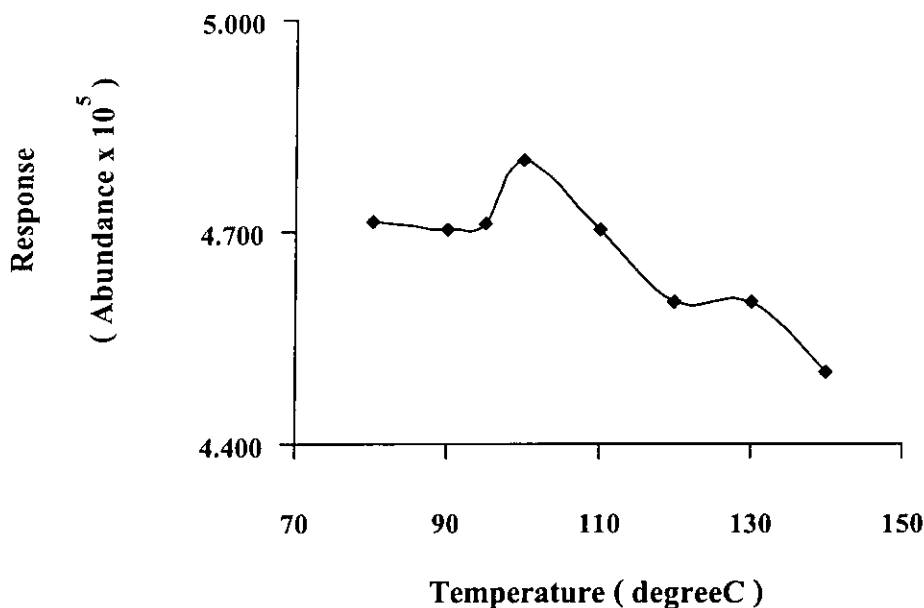


Figure 9 Relative response of MSD detector to various initial temperatures

Step 2: The hold time for initial temperature

The hold time for initial temperature was studied with the temperature program as shown in Figure 9

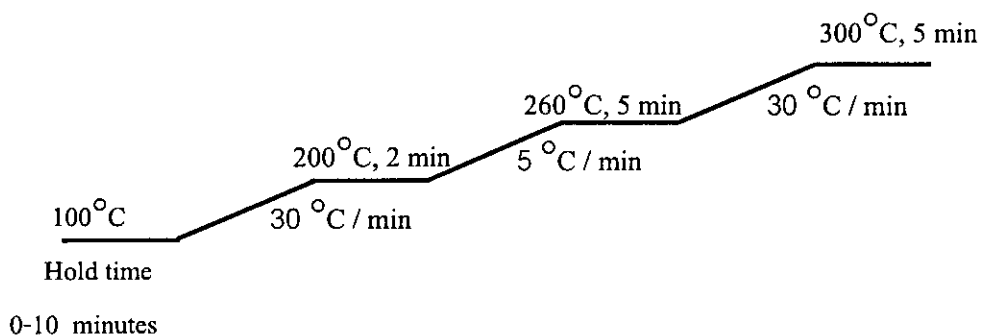


Figure 10 Temperature programming in step 2

The results of the responses at various hold times (0 – 10 minutes) are shown in Table 9 and Figure 11. The hold time of 3 minutes provided the highest response. It provided 21 % more response than at 0 minute hold time while analysis time only took 3



minutes longer. Thus, the 3 minutes hold time of initial temperature was chosen since it provided significant response improvement.

Table 9 Relative response of detector to various hold times for initial temperature

Hold time ( minutes )	Response* ( Abundance )	Analysis times ( minutes )
0	287884	22.00
2	318931	24.00
3	349698	25.00
4	331503	26.00
6	324218	28.00
8	292043	30.00
10	273721	32.00

\*mean of 5 replications, RSD < 4 %

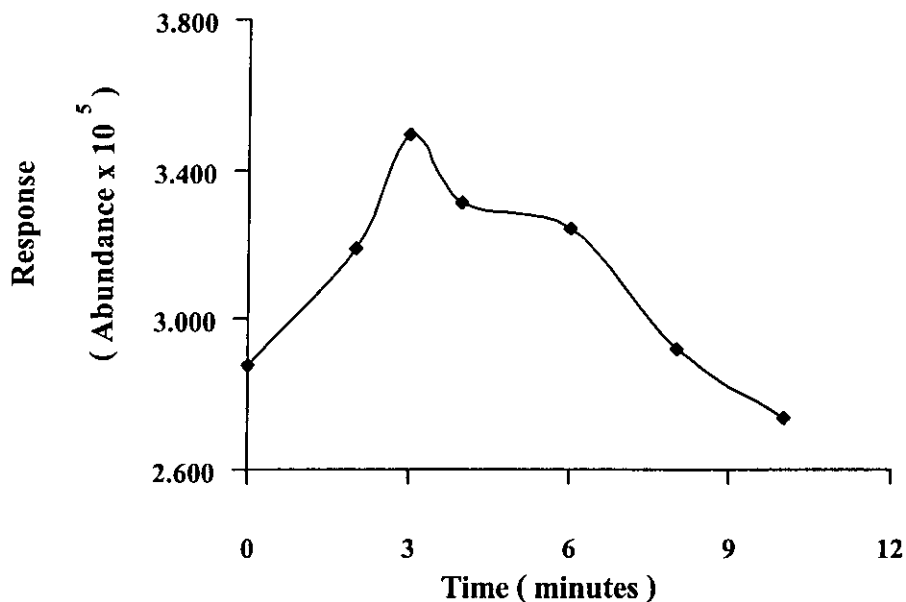


Figure 11 Relative response of detector to various hold times for initial temperature

### Step 3: The first ramped rate

Capillary column has been facilitated with the available of the cross-linked phases that are very stable under the fast temperature programming conditions. Although fast heating is possible the rate should not be more than  $35^{\circ}\text{C}/\text{min}$  to avoid the baseline drift (drift is a slow, constant directional change of the baseline over time similar to the entire chromatogram). Thus, only the ramp rates between 20 to  $35^{\circ}\text{C}/\text{min}$  were considered. The first ramp rate of temperature was studied in program 3 as shown in Figure 12. The purpose of this step was to reach the point before the boiling point of dioxin ( $240^{\circ}\text{C}$  at 18.15 psi, calculated from chromatogram). Since the ramp rate would not affect the elution of dioxin from column. So a fast ramp rate could be used to lower the analysis time.

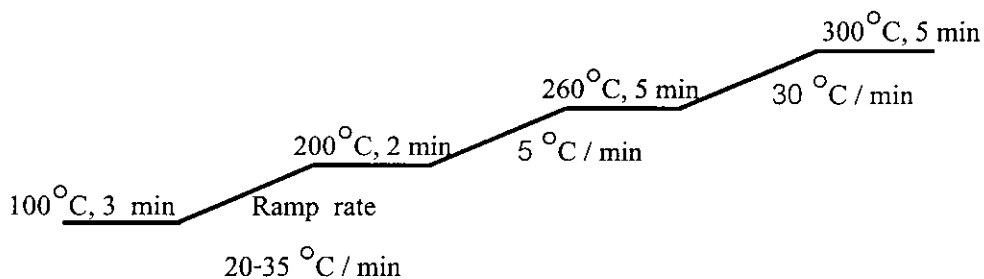


Figure 12 Temperature programming in step 3

The results are shown in Table 10 and Figure 13. The response was highest at  $30^{\circ}\text{C}/\text{min}$  with a low analysis time. This optimum first ramp rate was in agreement with the fast first ramp rate found in other works, for example, Hashimoto *et al.* (1995) and Abad *et al.* (1997).

Table 10 Relative response of the detector to various first ramped rates

Ramp ( $^{\circ}\text{C} / \text{minutes}$ )	Response* (Abundance)	Analysis time (minutes)
20	325204	26.00
25	329360	25.67
30	334868	25.00
35	334661	24.53

\*mean of 5 replications, RSD < 4 %

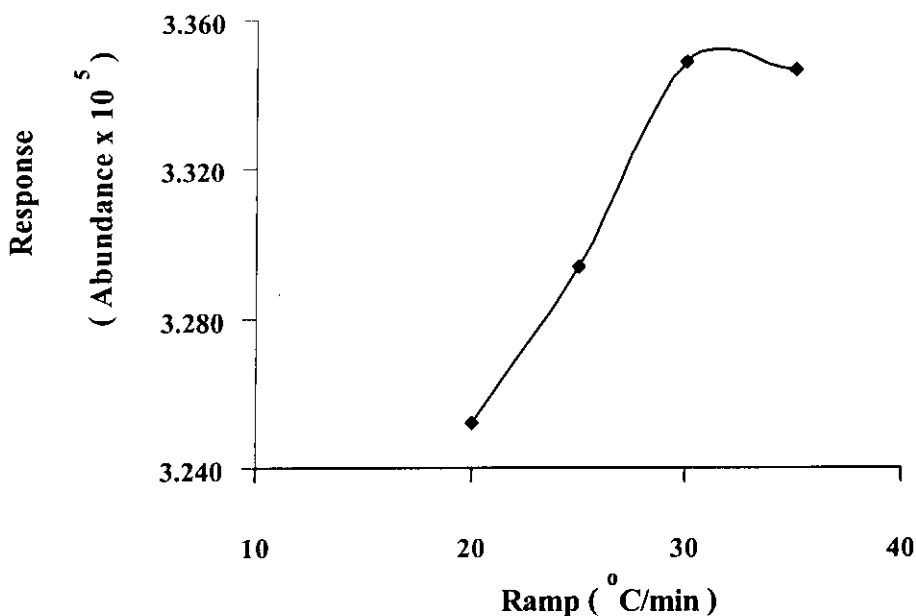


Figure 13 Relative response of the detector to various first ramped rates

#### Step 4: The second program temperature

The optimum second program temperature was obtained by the study in experiment 2.2.1.2. as shown in Figure 14 and the results are shown in Table 11 and Figure 15. The responses at the second temperatures between 210 - 220  $^{\circ}\text{C}$  were only slight different where 220  $^{\circ}\text{C}$  provided the best performance. Therefore, the optimum second temperature was chosen as 220  $^{\circ}\text{C}$ . In this step, there was a co-eluted peak (not baseline resolution peak) occurred when temperature was run at 210, 215  $^{\circ}\text{C}$  and 225  $^{\circ}\text{C}$ . Because the

second temperature affected on starting dioxin elution, it also affected on baseline resolution.

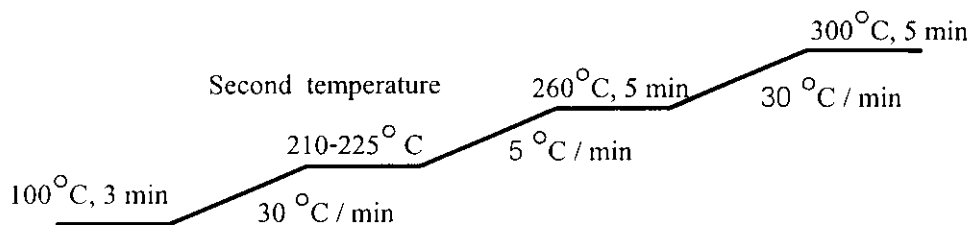


Figure 14 Temperature programming in step 4

Table 11 Relative response of the detector to various second program temperatures

Second temperature (° C)	Response* ( Abundance )	Analysis time ( minutes )
210	397641	23.34
215	400210	22.50
220	408227	21.67
225	321388	20.84

\*mean of 5 replications, RSD < 4 %

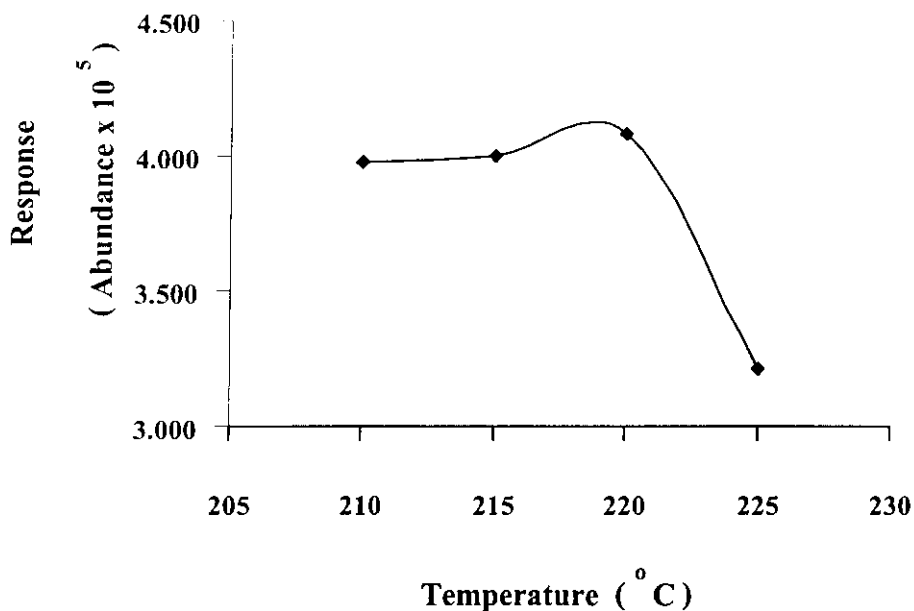


Figure 15 Relative response of the detector to various second program temperatures

Step 5: The second program temperature holding time

The second program temperature holding time was investigated in experiment 2.2.1.2, program 5, as shown in Figure 16.

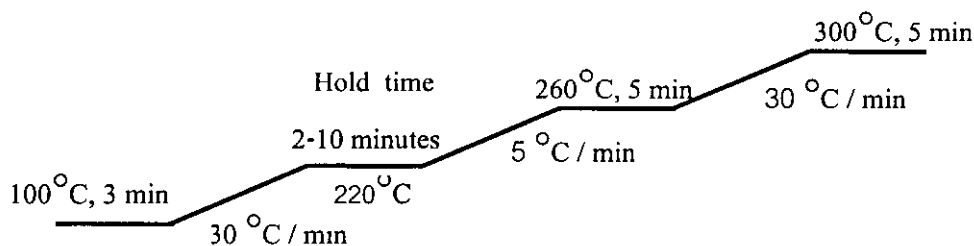


Figure 16 Temperature programming in step 5

The results showing the response at various holding times (2-10 minutes) of the second program temperature are in Table 12 and Figure 17. As the hold time of the second program increased, the response decreased. When 0 and 1 minute hold time were used, the co-eluted peak of TCDD appeared. Thus, the 2 minutes hold time of the second temperature program was chosen because it gave the highest response by resolution peak with the shortest analysis times.

Table 12 Relative response of the detector to second program temperature hold times

Hold time ( minutes )	Response* ( Abundance )	Analysis time ( minutes )
2	343950	21.67
4	333427	23.67
6	326050	25.67
8	315767	27.67
10	307335	29.67

\*mean of 5 replications, RSD < 4 %

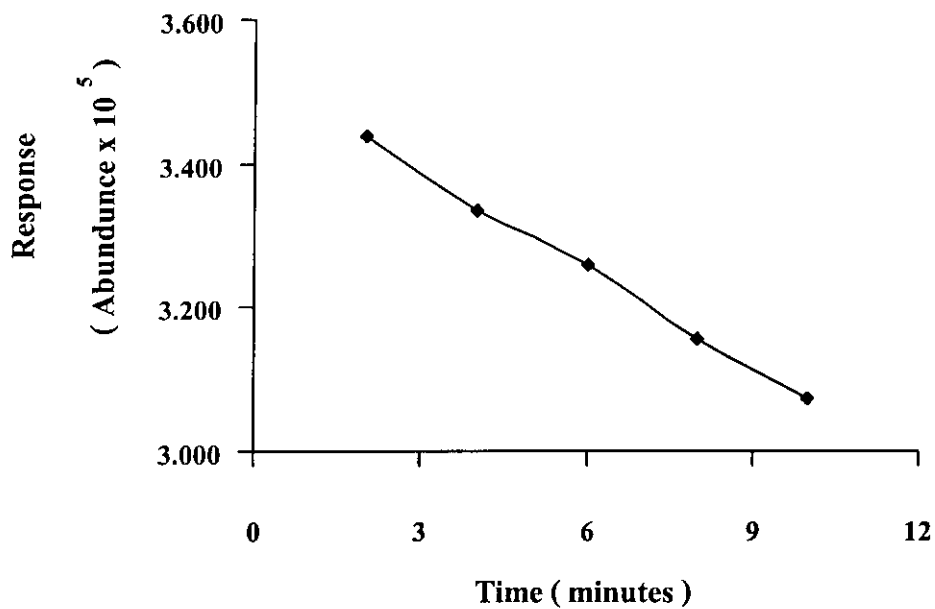


Figure 17 The relative detector response to various hold times of second program temperature

### Step 6: The second ramp rate

The second ramp rate of temperature in program 6 was studied from the experiment in 2.2.1.2. as shown in Figure 18. Since this step was to elute TCDD from the column a slow ramp rate should be used to improve the resolution.

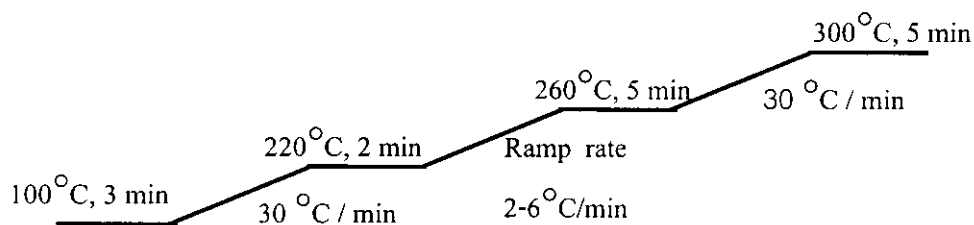


Figure 18 Temperature programming in step 6

The results are shown in Table 13 and Figure 19. The responses were different at various second ramp rates where 5 °C / min provided the highest response with the best performance. This optimum second ramp rate agreed with other works, for example, Hashimoto *et al.* (1995) and Abad *et al.* (1997) i.e. it should be a slow second ramp rate.

Table 13 Relative response of the detector to various second ramp rates

Ramp (°C / minutes)	Response* ( Abundance )
2	298715
4	304401
5	307220
6	300764

\*mean of 5 replications, RSD < 4 %

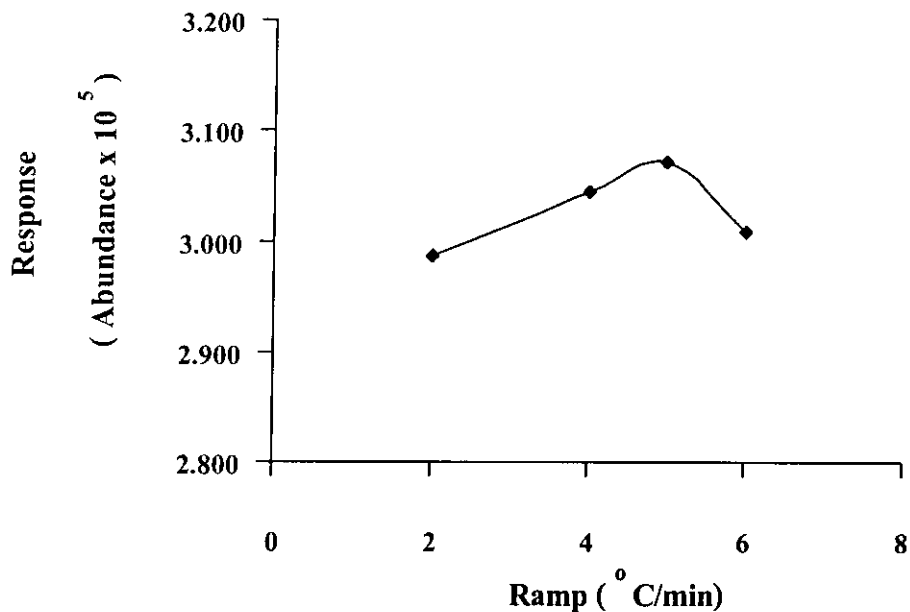


Figure 19 Relative response of the detector: various ramp rate to the third stage temperatures

Step 7: The third stage temperature program

The optimum third stage program temperature was obtained by the study in experiment 2.2.1.2. as shown in Figure 20 and the results are shown in Table 14 and Figure 21.

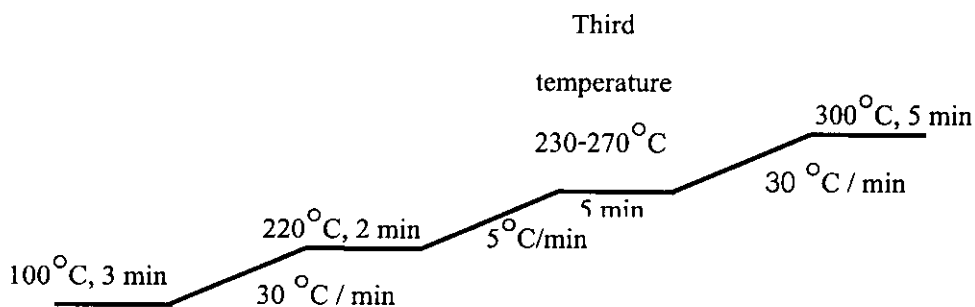


Figure 20 Temperature programming in step 7

The results showed a slight different of the responses at various third stage temperatures where 240°C was the best. The response slightly increased when the



temperature increased from 230 to 240 °C. But the response decreased when the temperature increased from 240 to 270 °C. This optimum third stage temperature was in agreement with Hashimoto *et al.* (1995) and Abad *et al.* (1997).

Table 14 Relative response of the detector to various third stage temperatures

Third temperature (° C)	Response* ( Abundance )
230	531274
240	535039
250	530896
260	527281
270	526541

\*mean of 5 replications, RSD < 4 %

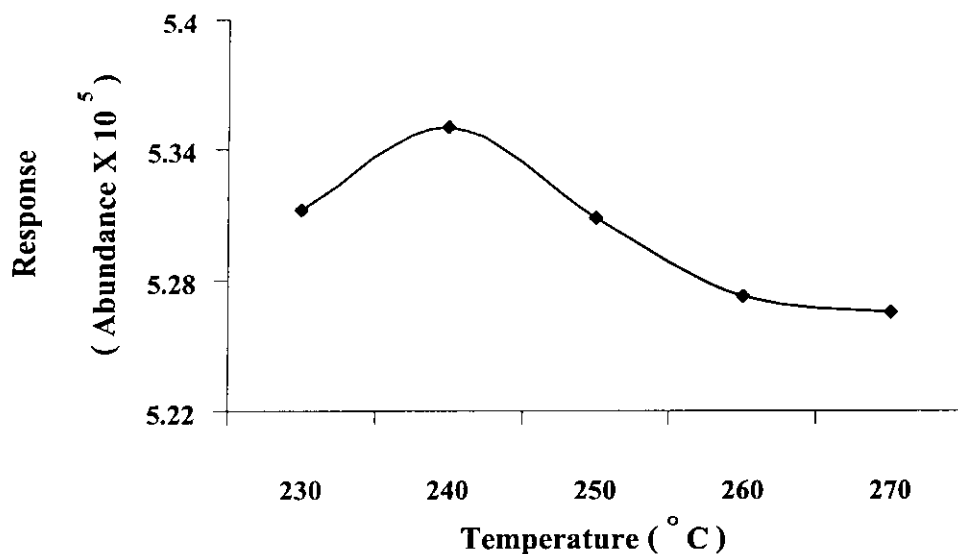


Figure 21 Relative response of the detector to various third stage temperatures

Step 8: The third stage program temperature hold time

The optimum third stage program temperature hold time was obtained by 2.2.1.2. as shown in Figure 22.

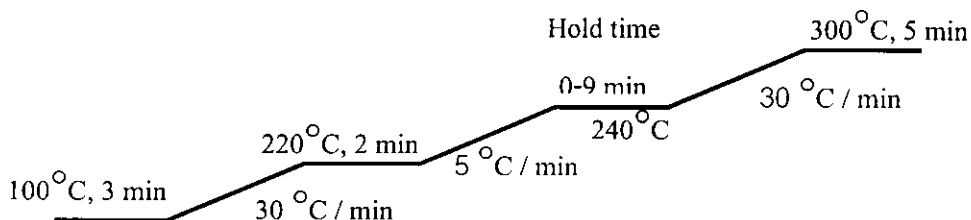


Figure 22 Temperature programming in step 8

The results (Table 15 and Figure 23) showed the different responses using various hold times (0 – 9 minutes). As the hold time of the third stage program temperature increased, the response decreased. When the hold time was 5 minutes, the detector provided the highest response.

Table 15 Relative response of the detector to various third stage program temperature hold times

Hold time (minutes)	Response* (Abundance)
0	269659
1	251347
3	227547
5	280080
7	218251
9	204365

\*mean of 5 replications, RSD < 4 %

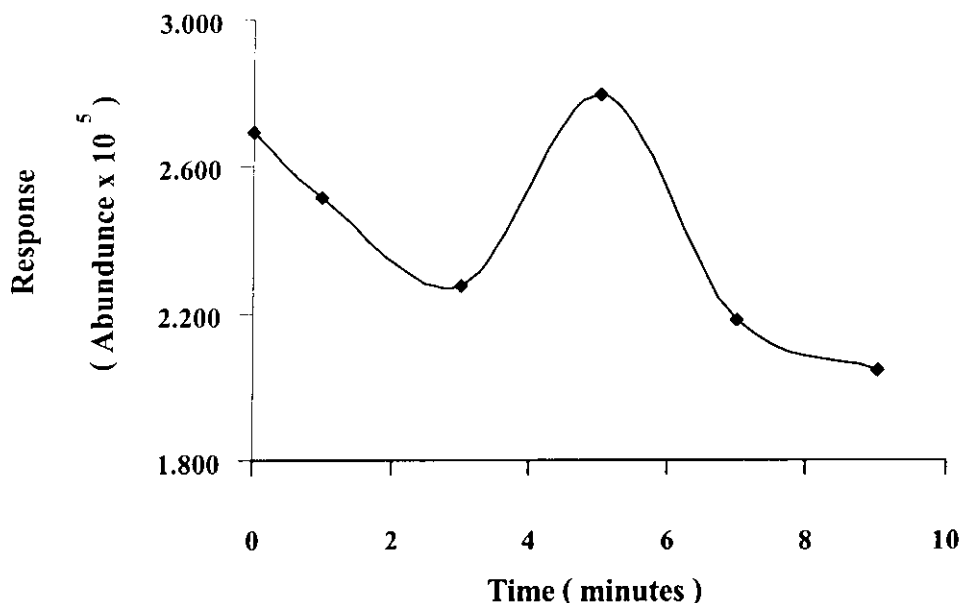


Figure 23 Relative response of the detector to various third stage program temperature hold times

Step 9: The third ramped rate

The optimum third ramped rate was obtained by 2.2.1.2. as shown in Figure 24 and the results are shown in Table 16 and Figure 25

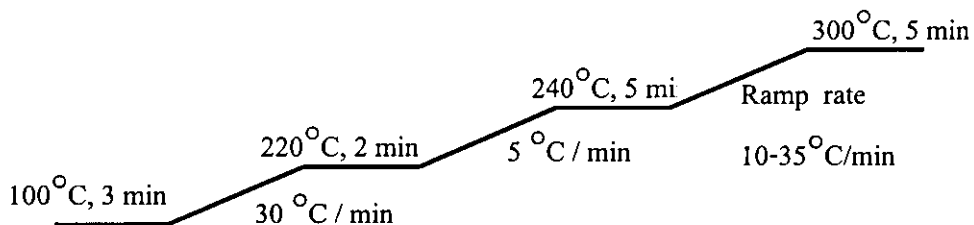


Figure 24 Temperature programming in step 9

The temperature in this stage was used to elute other components out of the column. This was to clean up the column before a new analysis. The ramp rate of 20<sup>o</sup>C/min provided the highest response and low analysis time. Therefore, the third ramped rate of 20<sup>o</sup>C/min was chosen for the optimum value.

Table 16 Relative response of the detector to various third ramped rates

Ramp ( $^{\circ}\text{C} / \text{minutes}$ )	Response* ( Abundance )	Time consumption ( minutes )
10	171958	29
15	175521	27
20	199366	26
25	192077	25
30	192343	25
35	180462	24

\* mean of replications.RSD < 4 %

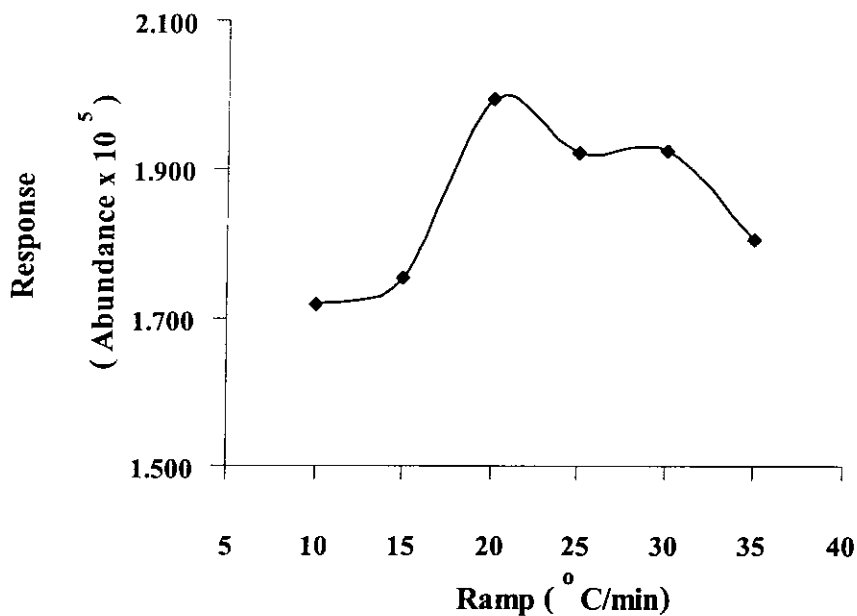


Figure 25 Relative response of the detector to various third ramped rates

The optimized temperature program ( Figure 26 ) was then used to analyze 1 ppb of standard TCDD, 2,3,7,8- tetrachlorodibenzo-p-dioxin, and the chromatogram is shown in Figure 27

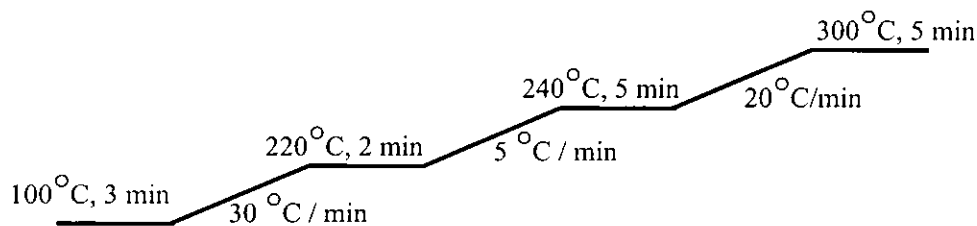


Figure 26 The optimized program temperature

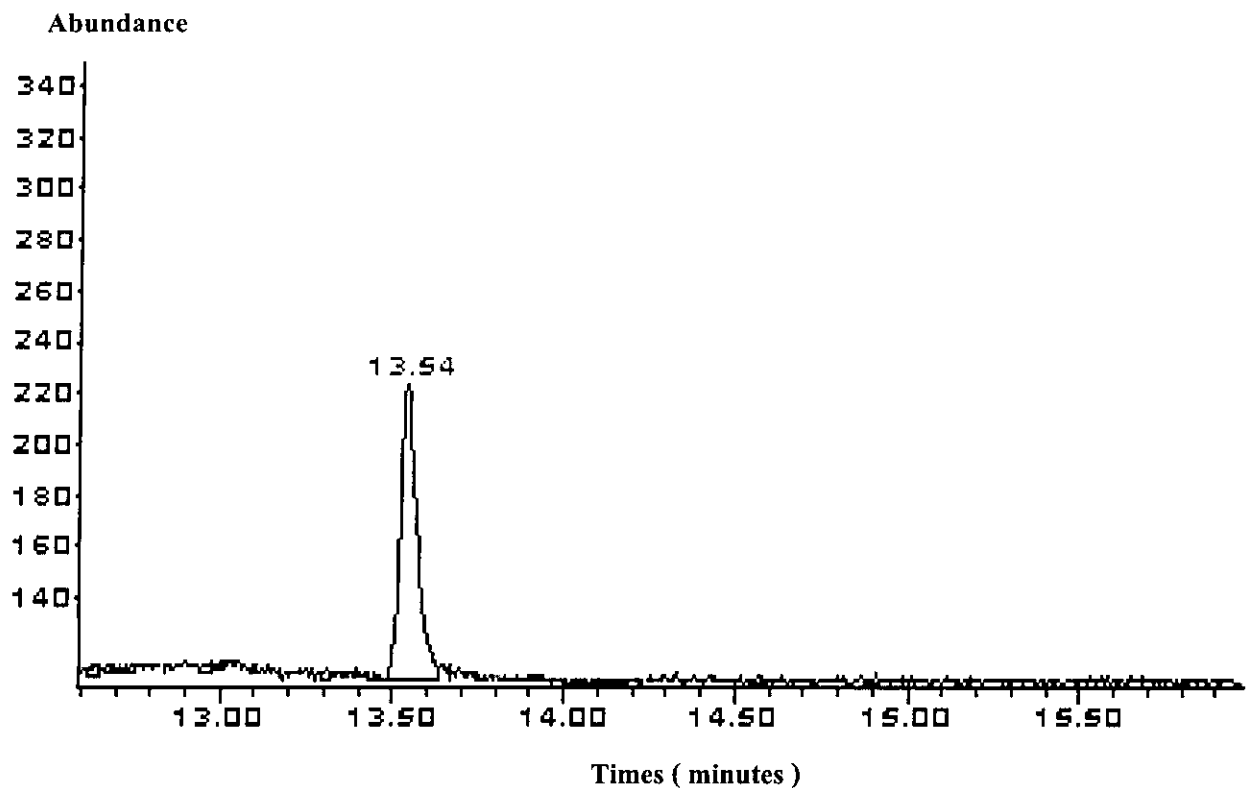


Figure 27 Chromatogram of 1 ppb Dioxin (TCDD)

### 3.1.3 Inlet temperature

The inlet temperature is an important parameter since it must be high enough to vaporize the whole sample. In most GC the inlet systems was constructed by some mechanical and electrical parts to make inlet temperature high enough to vaporize instantaneously all components in a sample without decomposition, condensation and minimum dead volumes to avoid diffusion of the sample in the mobile phase. Experiment 2.2.1.3 studied the effect of the inlet temperature and the results are shown in Table 17 and Figure 28. The response increased by 12% as the temperature increased from 260 °C to 280 °C and decreased when the inlet temperature were higher. The inlet temperatures of 280 °C was chosen since it completed the vaporization of the whole sample. The result from this work, 280 °C, agreed with Abad *et al.*(1997) i.e. 275 °C.

Table 17 Relative response of the detector to various inlet temperatures

Temperature ( ° C )	Response* ( Abundance )
260	103846
270	109457
280	116121
290	114404
300	113241
310	111203

\*mean of 5 replications, RSD < 4 %

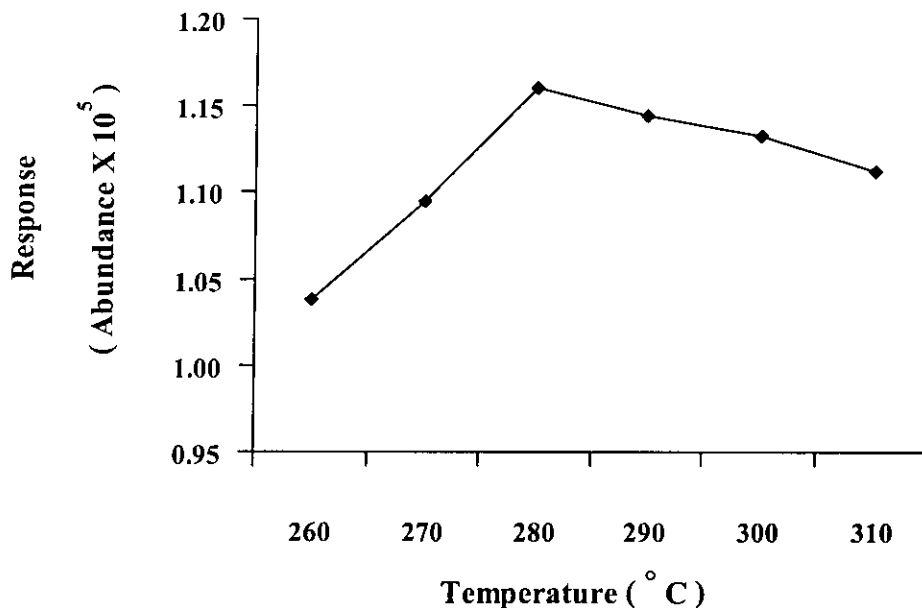


Figure 28 Relative response of the detector to various inlet temperatures

### 3.1.4 Interface temperature

The interface portion has to maintain the vaporization of TCDD exited from the GC column to the ion source of the mass spectrometer, interface temperature must be maintained at the temperature greater or equal to 300 °C (2.2.1.2) during analysis to prevent the condensation of less volatile compounds (US EPA, 1994). The interface temperature was investigated from 280 °C to 300 °C (2.2.1.4). The upper limit of 300 °C was set because the column temperature was limited to a maximum temperature of 305 °C. The results are shown in Table 18 and Figure 29. The response increased as the interface temperature increased and 300 °C was then chosen.

Table 18 Relative response of the detector to various interface temperatures

Temperature ( ° C )	Response* ( Abundance )
280	156686
290	168921
300	175769

\*mean of 5 replications, RSD < 4 %

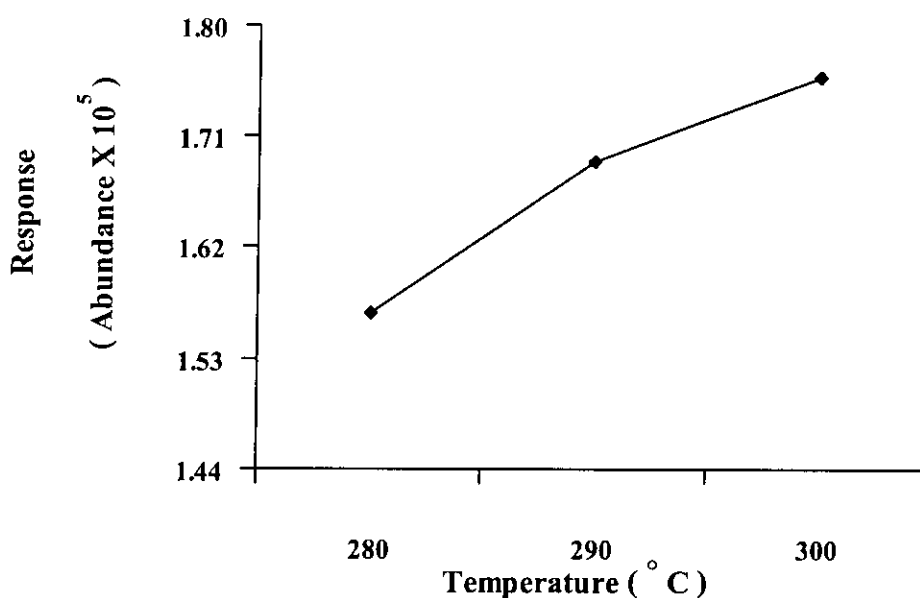


Figure 29 Relative response of the detector to various interface temperatures

### 3.2 Linear dynamic range

Linear dynamic range or linearity is the sample concentration range over which the detector response is linear. This is the method detectable amount up to the upper concentration level which produces a deviation from linearity ( Grob, 1985 ). Table 19 and Figure 30 showed responses at various concentrations with the relative standard deviation ( RSD ) of less than 4 % for 5 replicates. The results show that TCDD response to mass selective detector has a wide linear dynamic range of 0.5 – 100.0 ng / mL or their power was nearly 4. The results agreed well with Brochu *et al.* (1992) and the specification of Agilent 5973 Mass selective detector model ( Agilent 1996 ).



Table 19 Relative response of the detector to various concentrations

Concentration ( ng / mL )	Response* ( Abundance )
0.5	4683.0
0.7	7336.0
0.8	8188.0
1.0	9473.0
5.0	33010.0
10.0	56159.0
20.0	139960.6
30.0	219314.4
40.0	304049.8
50.0	394766.6
60.0	484066.3
70.0	545995.8
80.0	640531.0
90.0	745524.6
100.0	837510.4

\*mean of 5 replications, RSD < 4 %

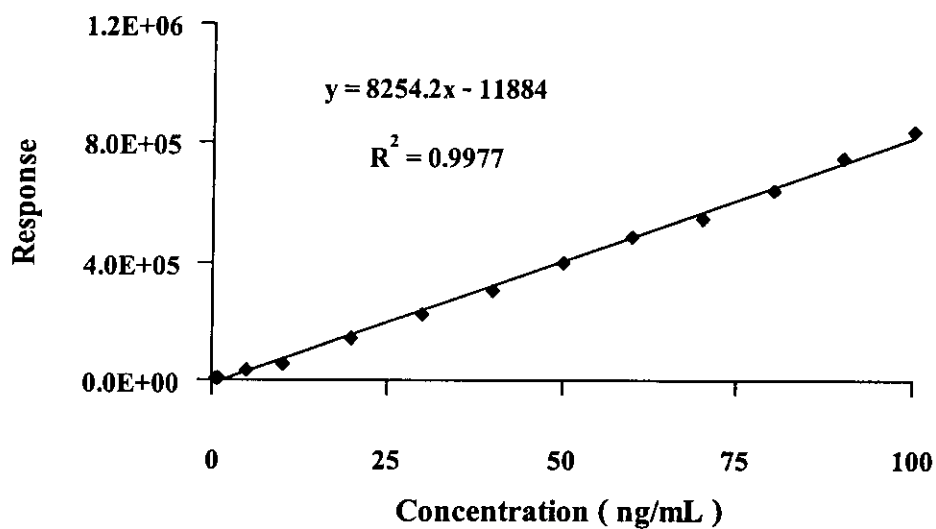


Figure 30 Relative response of the detector to various concentrations

### 3.3 Detection limit

The detection limit was obtained by experiment 2.2.3 followed the IUPAC method ( Long and Winefordner, 1983 ). The gas chromatography was operated at optimum conditions i.e. inlet temperature 280 ° C, interface temperature 300 ° C, ion source temperature 230 ° C, carrier flow rate 1 mL / min, and temperature programming of program 9 as in 2.2.1.2. TCDD standard concentrations ( 0.5, 1.0, 5.0 and 10.0 µg / L ) was injected to the system. The calibration curve was then created by plotting peak area against concentrations. The slope of the curve ( m ) was 0.9977. Next the responses of 30 blanks,  $X_B$ , was measured and the standard deviation of concentration was determined, i.e. 5.63. From equation 3 in 2.2.3, detection limit,  $C_L$  could be calculated that is

$$C_L = kS_B / m$$

$$\text{Where } k = 3$$

$$S_B = 5.63$$

$$M = 0.9977$$

$$C_L = 3 \times 5.63 / 0.9977$$

$$C_L = 16.9 \text{ ng / L}$$

This detection limit was higher than that of other work( Taylor *et al*, 1995 ) which was based on the gas chromatography - tandem mass spectrometry ( GC/MS/MS ). The detection limit was 1 ng/L. The higher detection limit in this work was probably due to the different in the system i.e. in this work it was a gas chromatography - low resolution mass spectrometry.

### 3.4 Optimization of sample preparation step

The Amberlite XAD-2 was prepared as described in 2.3.1 of Chapter 2 and was loaded by 4 ng standard dioxin spiked water. The extraction was done by ultrasonic extraction as described in 2.3.2. Then, 4 mL of aliquot was obtained for GC-MS analysis under the optimum conditions (3.1.4.). The identification of dioxin was based on the retention time and the ratio of the responses at the  $M^+$  and  $(M+2)^+$  values on the SIM chromatograms (Hashimoto *et al.*, 1995). There were 6 parameters affecting the extraction efficiency that needed to optimize: 1) sequencing of conditioning solvents series, 2) extraction solvent, 3) extraction time, 4) volume of extraction solvent, 5) numbers of extraction, 6) volume of spiked water.

#### 3.4.1 Sequencing of conditioning solvents series

Amberlite XAD-2 resin was conditioned prior to use to remove all traces of preservative and residual monomeric compounds (Supelco 1997). Following the reports of Lohmann *et al.* (2000) and Yang *et al.* (1999) two series of sequencing of conditioning solvents were used (2.3.3.1) and the results were shown in Table 20. The second series provided slightly higher extraction efficiency than the first ones with 6 % RSD. Both series could be used as the sequencing conditioning solvents. However the second series (methanol-water) only require 1 hour of the preparation time, one half of the first series. Thus, the series of methanol-water system was chosen for conditioning solvent to prepare the XAD-2 resin.

Table 20 Extraction efficiency of sequencing solvent series

Series No	Series of sequencing solvent	Extraction efficiency	Preparation time
1	methanol-acetone-toluene-acetone- methanol-water	60 %	2 hours
2	Methanol-water	63 %	1 hour

\*mean of 3 replications, RSD < 8 %

### 3.4.2 Extraction solvent

The three systems of extraction solvent i.e. hexane-acetone ( 1:1, v/v ) ( Lohmann, *et al.*, 2000 ), toluene, and toluene-acetone ( 1:1, v/v ) ( Yang, *et al.*, 1999 ) were studied (experiment 2.3.3.2). The results showed that toluene-acetone ( 1:1, v/v ) was the best extraction solvent as shown in Table 21. By considering the structure of TCDD, it consists of an aromatic phenyl core while toluene is aromatic, hexane is aliphatic hydrocarbon molecule. Thus, TCDD is more soluble in toluene than in hexane due to the polarity. This led to the higher extraction efficiency of toluene and toluene-acetone than hexane-acetone. Comparing toluene and toluene-acetone, the latter gave a slightly higher extraction efficiency. It was also better suited since it helped to remove the resin off the glass column.

Table 21 Extraction efficiency of various extraction solvent

Extraction solvent	Extraction efficiency
Hexane-acetone	31
Toluene	68
Toluene - acetone	69

\*mean of 3 replications, RSD < 4 %

### 3.4.3 Extraction time

The extraction time for ultrasonic extraction was obtained by the experiment in 2.3.3.3. From the results in Table 22, extraction efficiency increased as the extraction times increased from 10 to 20 minutes. When the extraction time got longer the extraction efficiency decreased. It could be that the high extraction time could attack the eluted TCDD molecules and destroy the adsorbate molecule of each microspheres ( Kimura, *et al.*, 2001 ). Since the extraction time of 20 minutes provided the high extraction efficiency i.e. 68% with only 3%RSD, this was chosen to be the optimum extraction time.

Table 22 Extraction efficiency of various extraction time

Extraction time ( minutes )	Extraction efficiency
10	34
20	68
30	37
40	34

\*mean of 3 replications, RSD < 9 %

#### 3.4.4 Volume of extraction solvent

Volume of solvent was studied for elution completeness and to achieve the high extraction efficiency. The semi-micro extraction was used for this study to reduce cost and amount of hazardous of waste. Solvent volumes of 30, 40, 50, 60, and 70 mL were tested in 2.3.3.4. and the results are shown in Table 23. The volume of 60 mL ( toluene-acetone, 1:1,v/v ) provided the maximum extraction efficiency, 72 % with the relative standard deviation of 6 %.

Table 23 Extraction efficiency of various volume of solvent

Volume of solvent	Extraction efficiency
30	60
40	58
50	58
60	72
70	71

\*mean of 3 replications, RSD < 9 %

### 3.4.5 Numbers of extraction

Numbers of extraction was investigated to enhance the extraction efficiency of the 60 mL solvent volume. Single, double and triple extractions were studied in the experiment 2.3.3.5.

The results are shown in Table 24, the average extraction efficiency of TCDD with double (2 X 30 mL) and triple (30 mL and 2 X 15 mL) extractions was 93% (6%RSD) and 104% (8% RSD), respectively. The extraction efficiency of the double and triple extractions were not much difference, but triple extraction took 20 minutes longer than the double extraction (40 minutes). The results (Table 25) also indicated that the triple extraction of blank sample was more contaminated than double extraction. So the double extraction was chosen for further studies.

Table 24 Extraction efficiency of different number of extractions

Number of extractions	Extraction efficiency	Time consumption (minutes)
1	70	20
2	93	40
3	104	60

\*mean of 3 replications, RSD < 8 %

Table 25 Contaminated concentration from blank sample using different number of extractions

Number of extractions of blank sample	Contaminated Concentration, ng / L
1	6.90
2	20.58
3	32.92

\*mean of 3 replications, RSD < 8 %

### 3.4.6 Volume of spiked water

Preliminary study using spiked technique (spiked 40  $\mu\text{L}$  100 ng/mL standard) in 25 gram conditioned XAD-2 resin indicated that the extraction efficiency was less than 50%. It could be that most of the TCDD wasn't trapped by XAD-2. To solve this problem, the optimum volume of TCDD water sample was investigated after other parameters were optimized. This was studied in experiment 2.3.3.6. The results are shown in Table 26, the extraction efficiency varied with the volume of water. It was shown that 100 mL volume water provided the highest extraction efficiency, 95% (1%RSD).

Table 26 Extraction efficiency when using different volume of the TCDD water sample

Volume of TCDD water sample, mL	Extraction efficiency
100	95
200	85
400	80
600	41
800	52
1000	67

\*mean of 3 replications, RSD < 9 %

### 3.5 Qualitative and Quantitative analysis

Water samples were collected from the following sampling sites:

Site 1 Hatyai Regional Water Supply

Site 2 Songkhla Monitoring Municipal Landfill - location A

Site 3 Songkhla Monitoring Municipal Landfill - location B

The water samples were prepared using the optimum conditions, then analyzed by GC-MS also using optimum conditions. Their concentration were calculated from the chromatogram identification of dioxin based on the retention time and the ratio of the responses at the  $M^+$  and  $(M+2)^+$  values on the SIM chromatograms. The results from the experiments (2.3.4) are shown in Table 27. Their concentrations could not be

determined because they were less than the detection limit of 16.9 ng/L. That is TCDD was not detectable by the external standard method. Further analysis was then carried out by standard addition method with the same samples. The results of the standard addition method of each sample are shown in Table 28-30 and Figure 31-33. The TCDD concentration were determined and corrected by subtracting with the result from the blank sample in Table 25 and these are shown in Table 31.

Table 27 Concentration of water samples

<b>Sample no.</b>	<b>Concentration, ng/L</b>
1	N.D.
2	N.D.
3	N.D.

N.D. = non detectable, i.e. concentration was less than the detection limit of 16.9 ng/L



Table 28 Standard addition method of Sample No. 1: Hatyai Regional Water Supply

Spiked concentration, ng/L	Response ( Abundance x 10 <sup>3</sup> )
0	83
600	3846
780	4851
960	6163

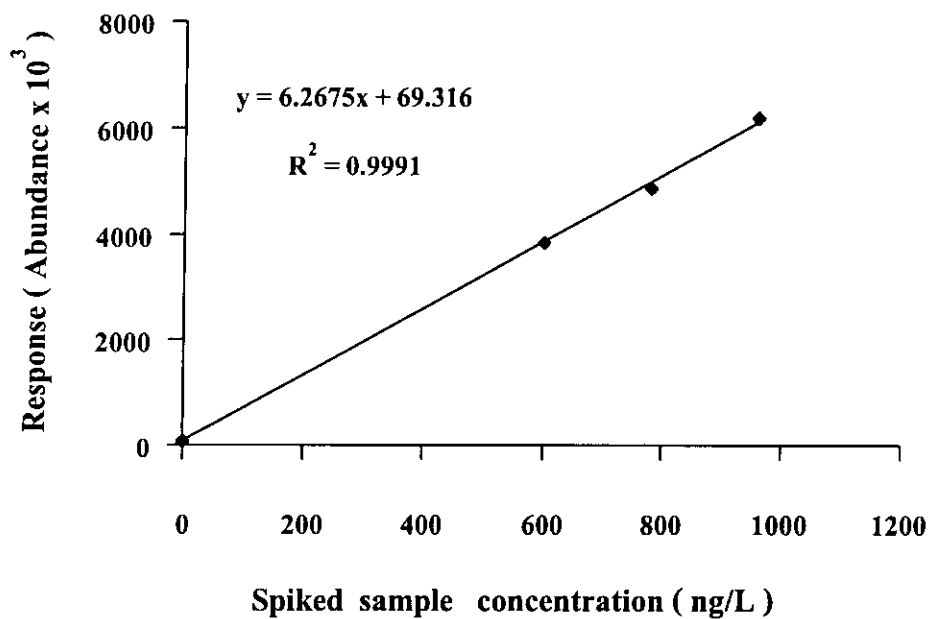


Figure 31 The standard addition curves of TCDD for Sample No. 1

Table 29 Standard addition method of Sample No. 2: Location A-Songkhla Monitoring  
Municipal Landfill

Spiked concentration, ng/L	Response ( Abundance x 10 <sup>3</sup> )
0	489
600	6101
780	7712
960	9266

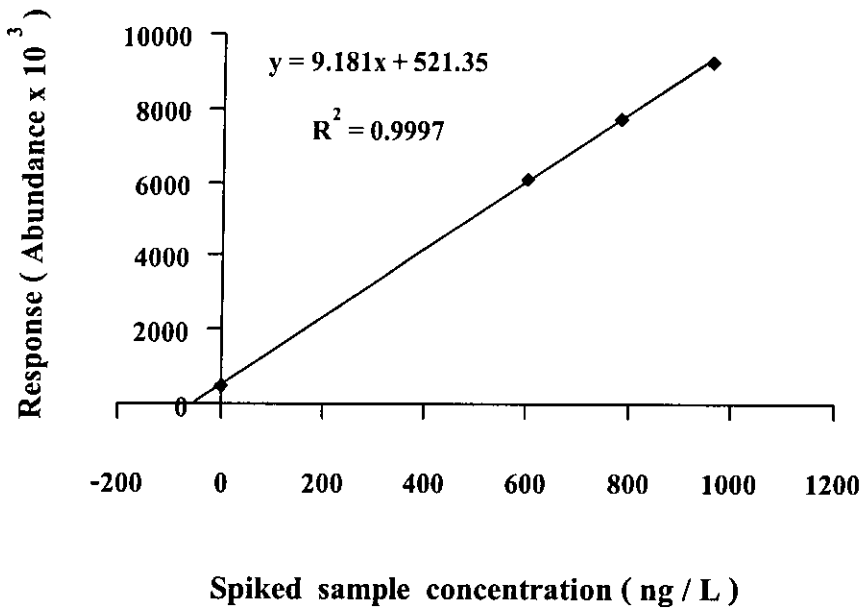


Figure 32 The standard addition curves of TCDD for Sample No. 2

Table 30 Standard addition method of Sample No. 3: Location B-Songkhla Monitoring  
Municipal Landfill

Spiked concentration, ng/L	Response ( Abundance x 10 <sup>3</sup> )
0	113
600	4020
780	4957
960	6141

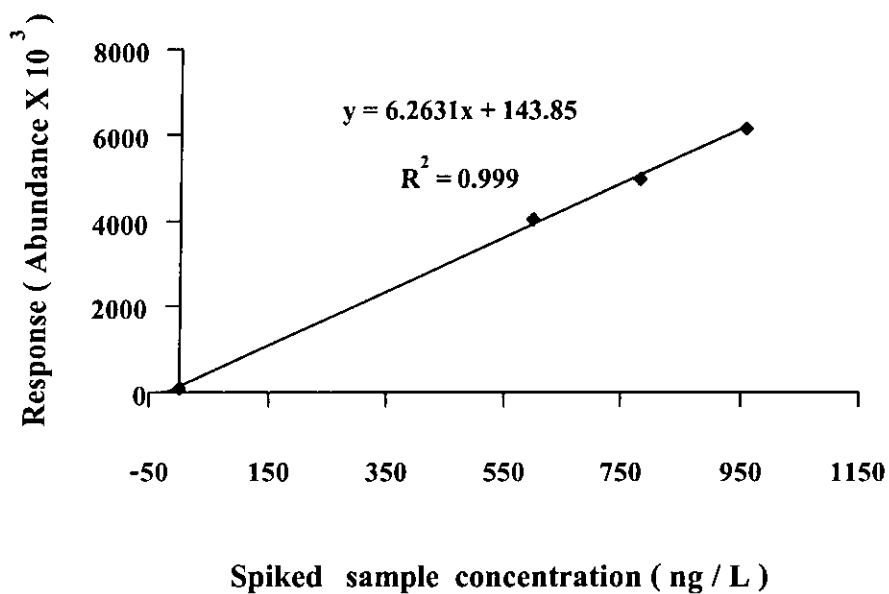


Figure 33 The standard addition curves of TCDD for Sample No. 3

Table 31 TCDD concentrations of the samples determined by standard addition method

Sample No.	Concentration, ng / L
1	Not detectable
2	16.2
3	2.3

The analysis of TCDD by standard addition method found that the concentration of TCDD in water sample were in the range of non-detectable - 16.2 ng/L. These were all lower than 16.9 ng/L, the detection limit and, therefore, was not detected without using the standard addition method.